

YAMAGATA-HET-96-14

KYUSHU-HET-37

SAGA-HE-115

Jan., 1997

Phase Structures of $U(2)$ Gauge Theory with θ -Term in 2 dimensions

Masahiro IMACHI*, Takaaki KAKITSUKA**, Norimasa TSUZUKI***

and

Hiroshi YONEYAMA†

**Department of Physics, Yamagata University, Yamagata 990, Japan*

***NTT Opto-Electronics Laboratories, Atsugi, Kanagawa 243-01, Japan*

****Department of Physics, Kyushu University, Fukuoka 812, Japan*

† *Department of Physics, Saga University, Saga 840, Japan*

ABSTRACT

$U(2)$ lattice gauge theory with θ -term in 2 space-time dimensions is investigated. It has non-Abelian real action and Abelian($U(1)$ type) imaginary action. The imaginary action is defined as the standard θ -term. As the effect of renormalization group(RG) transformation, non-Abelian imaginary action is induced. After many steps of RG transformation, non-Abelian part will die away. After several steps of RG transformations, renormalized action approaches so called heat kernel action. Phase transition is found at $\theta = \pi$ only.

* e-mail:imachi@sci.kj.yamagata-u.ac.jp

** e-mail:kaki@aecl.ntt.co.jp

*** e-mail:tsuz1scp@mbox.nc.kyushu-u.ac.jp

† e-mail:yoneyama@cc.saga-u.ac.jp

§1. Introduction

Much progress has been made in the lattice gauge theory approach in these twenty years. The systems studied, however, are limited mostly to those without topological term($=\theta$ -term). This is due mainly to the difficulty to treat θ -term in numerical calculations in Euclidean space-time. Numerical calculations are performed with the use of probability weight defined by Euclidean action. When the system is limited to those without θ -term, the probability weight is given by positive quantity. But when θ -term is added to the Euclidean action, we obtain complex weight due to the nature that θ -term is a pure imaginary quantity in Euclidean space-time. The θ -term, however, is expected to lead to physically interesting effects.

In 4 space-time dimensions, θ -term leads to strong CP violation which is severely suppressed in real world, although it is not excluded from theoretical frame work. The system with θ -term leads to oblique confinement or rich phase structures [1][2] [3] .

In 3 space-time dimensions, it is called Chern-Simons term and is related to new physical effect, e.g., fractional statistics. In compact U(1) gauge theory, the system is in the confinement phase, as discussed by Polyakov due to the monopole excitation. There is a conjecture that the system undergoes a phase transition[4]. The system is in “deconfined phase” when θ -term is included since existence of θ -term has the effect to wash out magnetic monopoles and then the system cannot be in confined phase in arbitrary nonzero θ .

In two space-time dimensions, the compact U(1) system is in the confinement phase. The existence of θ -term however, leads to deconfinement phase transition when $\theta = \pi$ [5] [6][7].

The system with CP^{N-1} symmetry in 2 space-time dimensions has much similarity to 4 dimensional gauge systems(asymptotic freedom, confinement, topological excitations etc.) The study of CP^{N-1} with θ -term is quite interesting. Especially how θ -term affects the phase structures will be quite important. In the previous paper we numerically studied CP^1 model with θ -term in two dimensions, where we obtained θ - dependence of the partition function through the measurements of topological charge(Q) distribution $P(Q)$ [8]. The fourier transform of this distribution gives us the partition function $Z(\theta)$ [9]. We saw first order phase

transition in strong real coupling regions and weaker transition in weak coupling regions (but we could not conclude that it belongs to 2nd order phase transition).

Schierholz has pointed out that CP^{N-1} ($N = 4$) model in 2 dimensions undergoes first order transition at some values of θ , depending on the real coupling. In strong (real) coupling, θ_c is given by π and θ_c deviates from π at those β greater than some value. He conjectured that θ_c goes to zero at weak coupling limit ($a \rightarrow 0$). According to him, the continuum limit value of θ would be zero and this would be the dynamical explanation for the smallness of physical θ [10][11].

The study of CP^{N-1} system or gauge systems with θ -term will be quite important to understand really the reason of vanishingly small value of θ in four dimensional QCD. There will be various approach to study the system with θ -term. One of them is numerical simulation, where the difficulty of complex Euclidean action and thus complex Boltzmann weight is overcome by first obtaining topological charge(Q) distribution $P(Q)$ and then by calculating $Z(\theta) = \sum_Q P(Q) e^{i\theta Q/2\pi}$ [12]. Another method to study the phase structure is to apply real space renormalization group method to the system[13] [14] [15] [16]. In this approach, the information of the phase structure is obtained through the analysis of renormalization group flow of various couplings(β , θ etc.)[17].

In this paper we apply real space renormalization group method to 2 dimensional U(2) lattice gauge theory[18]. The reason to choose U(2) symmetry is that we are interested in the system with both non Abelian(SU(N)) and Abelian(U(1)) part. In order to have nontrivial θ -term we have to study the gauge group with Abelian part, because standard imaginary action $\text{Tr}\varepsilon_{\mu\nu}F_{\mu\nu}$ becomes nontrivial when gauge group has U(1) part. The symmetry SU(N), without U(1) part, on the other hand leads to trivial θ -term, since $\text{Tr}\varepsilon_{\mu\nu}F_{\mu\nu}$ is zero. So we have chosen U(N) symmetry. The group U(2) is the simplest among U(N) ($N \geq 2$)'s. In U(2) gauge symmetry, we will pay attention to the interplay between Abelian and non-Abelian SU(2) effects. To see nontrivial effect, we choose the real coupling term as the fundamental representation $\beta_{l_1 l_2} = \beta_{11}$ (l_1 and l_2 are U(1) and SU(2) part of U(2) symmetry, respectively and $l_1 = 1$ and $l_2 = 1$ means that the action belongs to fundamental representation of both U(1) and SU(2) part).

In the choice of θ -term action, there are two possibilities according to possible U(N) gauge invariants; $\det U$ and $\text{Tr}U$, where U is an element of U(N) group belonging to fundamental representation. One is “standard θ -action” which is defined

as $\frac{1}{2} \frac{\theta}{2\pi} (\ln \det U - \text{c.c.})$ corresponding to the continuum limit form $i \frac{\theta}{2\pi} F_{\mu\nu} \varepsilon_{\mu\nu}$. The other choice is “Wilson θ -action” defined as $\frac{1}{2} \frac{\theta}{2\pi} (\text{Tr} U - \text{c.c.})$ corresponding to imaginary version of “Wilson action” (real Wilson action is defined as $\frac{1}{2} \beta (\text{Tr} U + \text{c.c.})$).

In this way, bare actions we consider in this paper are given by

- (i) real action which has both U(1) and SU(2) part of U(2) group
- (ii) imaginary action which has only U(1) part.

We specify the irreducible representation (IR) of U(2) by two integers l_1 and l_2 corresponding to U(1) and SU(2) part, respectively. Trivial representation is given by $l_1 = 0$ and $l_2 = 0$. The set of real and imaginary couplings is denoted as $\beta_{l_1 l_2}$ and $\gamma_{l_1 l_2}$ respectively. Bare action is defined by

- (1) $\beta_{11} \neq 0$ and $\beta_{l_1 l_2} = 0$ for other representations and
- (2) bare imaginary action contains only U(1) part ((i) αx (standard θ -action) or (ii) $\alpha \sin x$ (Wilson θ -action) respectively), where x is defined as the U(1) variable of U(2) group ($\ln \det U - \ln \det U^\dagger = 2ix$ and $\text{Tr} U - \text{Tr} U^\dagger = 2i \sin x$).

In these actions, $\gamma_{l_1 l_2}$ with $l_2 \neq 0$ are zero.

Although bare imaginary action is given as the function of U(1) variable x only, the RG transformation induces nontrivial SU(2) part, and we have, for example, $\gamma_{11} \neq 0$ after RG transformations. On the other hand non zero β_{20} (originally zero) is induced as the RG effect. RG flow of (β_{20}, β_{40}) shows interesting behavior.

In the case of standard θ -term action, we find phase transition at $\theta = \pi$. The RG flow projected onto $(\beta_{20}$ and $\beta_{40})$ plane is controlled by a fixed point specified by $\theta = \pi$. For $\theta =$ very close to π but $\theta \neq \pi$, the RG flow is strongly affected by the $\theta = \pi$ fixed point, but after many steps of RG transformation, the RG flow finally goes to strong coupling fixed point $(\beta_{20}, \beta_{40}) = (0, 0)$.

Deconfinement transition at $\theta = \pi$ is limited to the coupling belonging trivial SU(2) representation and fundamental representation of U(1), i.e., β_{20} . The coupling belonging to non trivial SU(2) representation, e.g., β_{11} does not show deconfinement transition even at $\theta = \pi$.

§2. Formulation

§2.1 irreducible characters

In this paper we consider a gauge group, in 2 space-time dimensions, which has both non-Abelian part and θ -term(U(1) part). As the simplest of such group, U(2) group is adopted and interplay between Abelian and non-Abelian part will be investigated.

We denote the element of fundamental representation of U(2) group as U and

$$U = T\Lambda T^\dagger \quad (2.1)$$

where T is a unitary matrix diagonalizing U to Λ like

$$\Lambda = \begin{pmatrix} e^{i\phi_1} & 0 \\ 0 & e^{i\phi_2} \end{pmatrix} = e^{i\alpha_1/2} \begin{pmatrix} e^{i\alpha_2/2} & 0 \\ 0 & e^{-i\alpha_2/2} \end{pmatrix}. \quad (2.2)$$

Two parameters ϕ_1, ϕ_2 ($-\pi \leq \phi_1, \phi_2 \leq \pi$) of the diagonal part are replaced by two parameters α_1, α_2 as

$$\begin{aligned} \alpha_1 &= \phi_1 + \phi_2 \\ \alpha_2 &= \phi_1 - \phi_2. \end{aligned} \quad (2.3)$$

Characters $\text{Tr}U$ of general irreducible representations of U(2) group are given by

$$\chi_{\lambda_1\lambda_2}(\phi_1, \phi_2) = \Delta_{\lambda_1\lambda_2}(\phi_1, \phi_2) / \Delta_{00}(\phi_1, \phi_2) \quad (2.4)$$

where determinant is defined as

$$\Delta_{\lambda_1\lambda_2}(\phi_1, \phi_2) \equiv \det \begin{pmatrix} e^{i\phi_1(\lambda_1+1)} & e^{i\phi_1\lambda_2} \\ e^{i\phi_2(\lambda_1+1)} & e^{i\phi_2\lambda_2} \end{pmatrix} \quad (2.5)$$

and

$$\Delta = \Delta_{00} = \det \begin{pmatrix} e^{i\phi_1} & 1 \\ e^{i\phi_2} & 1 \end{pmatrix}. \quad (2.6)$$

Integers λ_1 and λ_2 denote the length of the first and the second row of Young tableau(see ref. Drouffe et al.[19]). Note that λ_1 and λ_2 are allowed to take both positive and negative values. Only constraint is $\lambda_1 \geq \lambda_2$. Dimension of IR is

$$d_{\lambda_1\lambda_2} = \lambda_1 - \lambda_2 + 1 \quad (2.7)$$

We will introduce another notation referring to U(1) and SU(2) part;

$$\begin{cases} l_1 = \lambda_1 + \lambda_2 \\ l_2 = \lambda_1 - \lambda_2 \end{cases} \quad (2.8)$$

$$\begin{cases} x = \alpha_1 = \phi_1 + \phi_2 \\ y = \alpha_2 = \phi_1 - \phi_2 \end{cases} \quad (2.9)$$

where $l_1(l_2)$ and $x(y)$ denotes the U(1)(SU(2)) part. As is evident from this definition, l_1 and l_2 are not completely independent but they obey constraints $l_1 + l_2 = \text{even integer}$ and $l_2 \geq 0$.

Explicit form of the character is

$$\chi_{l_1 l_2}(x, y) = e^{i \frac{l_1}{2} x} \frac{\sin(l_2 + 1) \frac{y}{2}}{\sin \frac{y}{2}} \quad (2.10)$$

$$d_{l_1 l_2} = \chi_{l_1 l_2}(0, 0) = l_2 + 1. \quad (2.11)$$

Two integers l_1 and l_2 denote $2q$ (q is ‘‘U(1) charge’’) and $2I$ (I denotes the magnitude of ‘‘isospin’’), respectively.

Invariant measure is given by[20]

$$d\Omega = dT \frac{1}{8\pi^2} d\phi_1 d\phi_2 \Delta \Delta^*, \quad (2.12)$$

where Δ^* is the complex conjugate of Δ .

Fundamental representation is defined as a single box in the Young tableau, i.e., $(\lambda_1, \lambda_2) = (1, 0)$, thus $(l_1, l_2) = (1, 1)$.

§2.2 Migdal Renormalization group

Partition function Z is defined as an integral

$$Z = \int d\Omega F(L, u)$$

at scale L . The integrand F is given by

$$F(L, u) = \exp(s(u) + iv(u)), \quad (2.13)$$

where u denotes an element of $U(2)$ group. This integrand F will be expanded by irreducible characters as,

$$F(L, u) = \sum_{l_1 l_2} d_{l_1 l_2} \chi_{l_1 l_2}(u) \tilde{f}_{l_1 l_2}(L). \quad (2.14)$$

Real and imaginary part of action $s(u)$ and $v(u)$, respectively, are also expanded into a series as

$$\begin{cases} s(L, u) = \sum_{l_1 l_2} \beta_{l_1 l_2} \left(\frac{\chi_{l_1 l_2}(u)}{d_{l_1 l_2}} - 1 \right) \\ v(L, u) = \sum_{l_1 l_2} \gamma_{l_1 l_2} \chi_{l_1 l_2}(u), \end{cases} \quad (2.15)$$

where $d_{l_1 l_2} = l_2 + 1$ is the dimension of IR(irreducible representation) (l_1, l_2) .

Using the orthonormality of the characters, RG transformation is defined[13]. Change of scale L to λL leads to

$$F(\lambda L, u) = \sum_{l_1 l_2} d_{l_1 l_2} \chi_{l_1 l_2}(u) (\tilde{f}_{l_1 l_2}(L))^{\lambda^2}. \quad (2.16)$$

After t steps of RG transformation,

$$F(\lambda^t L, u) = \sum_{l_1 l_2} d_{l_1 l_2} \chi_{l_1 l_2}(u) (\tilde{f}_{l_1 l_2}(l))^{\lambda^{2t}}. \quad (2.17)$$

The long distance behavior is determined by this equation at $t \rightarrow \text{large}$.

The change of coupling constants with scale transformation is determined by the character expansion of $F(\lambda L, u)$ as

$$F(\lambda L, u) = \exp \left\{ \sum_{l_1 l_2} \beta_{l_1 l_2}(\lambda L) \left(\frac{\chi_{l_1 l_2}(u)}{d_{l_1 l_2}} - 1 \right) + i \sum_{l_1 l_2} \gamma_{l_1 l_2}(\lambda L) \chi_{l_1 l_2}(u) \right\} \quad (2.18)$$

where left hand side is given by eq.(2.16). Equations (2.16) and (2.18) define the change

$$\{\beta_{l_1 l_2}(L), \gamma_{l_1 l_2}(L)\} \rightarrow \{\beta_{l_1 l_2}(\lambda L), \gamma_{l_1 l_2}(\lambda L)\} \quad (2.19)$$

and successive transformations give us the renormalization flow of coupling constants.

The real part of bare action is chosen as Wilson action with $\beta_{11}^b \neq 0, \beta_{l_1 l_2}^b = 0$ for all of other representations. For the imaginary part of the bare action, we can consider two possibilities;(1) “standard” imaginary action defined by

$$v_{\text{st}}(x) = i\alpha(\ln \det U - \ln \det U^\dagger)/2i = i\alpha x \quad (2.20)$$

and (2) “Wilson” imaginary action defined by

$$v_{\text{Wil}}(x) = i\alpha (\text{Tr } U - \text{Tr } U^\dagger)/2i = i\alpha \sin x, (\alpha \equiv \theta/2\pi). \quad (2.21)$$

Both of these approach $i\alpha x$ in the naive continuum limit.

In this paper standard imaginary action will be investigated. Due to the character expansion,

$$\begin{aligned} \text{“}x\text{”} &= i\left\{ -\chi_{20}(x) + \frac{1}{2}\chi_{40}(x) - \frac{1}{3}\chi_{60}(x) + \cdots \right. \\ &\quad \left. + \chi_{-20}(x) - \frac{1}{2}\chi_{-40}(x) + \frac{1}{3}\chi_{-60}(x) - \cdots \right\} \\ &= 2\left\{ \sin x - \frac{1}{2}\sin 2x + \frac{1}{3}\sin 3x - \cdots \right\}. \end{aligned} \quad (2.22)$$

Namely, the character expansion coefficient γ_{l0} of “ x ” is

$$\begin{cases} \gamma_{l0} = \frac{2i}{l}(-1)^{l/2}(l \neq 0) \\ \gamma_{00} = 0 \end{cases} \quad (\text{I})$$

where

$$\text{“}x\text{”} = \begin{cases} x - 2\pi & \text{for } \pi < x \leq 2\pi \\ x & \text{for } -\pi < x \leq \pi \\ x + 2\pi & \text{for } -2\pi \leq x \leq -\pi. \end{cases} \quad (2.23)$$

In the character expansion, we should be careful with the treatment of $x = \phi_1 + \phi_2$ and $y = \phi_1 - \phi_2$, because originally, ϕ_1 and ϕ_2 range over from $-\pi$ to π . We present an example of integration over Haar measure.

$$\tilde{f}_{l_1 l_2} = \int d\Omega \chi_{l_1 l_2}^*(x, y) F(x, y) = \tilde{f}_{l_1 l_2}^{(1)} + \tilde{f}_{l_1 l_2}^{(2)} \quad (2.24)$$

where

$$\tilde{f}_{l_1 l_2}^{(1)} = \int_{\pi}^{2\pi} dy (1 - \cos y) \int_{-2\pi+y}^{2\pi-y} dx F(x, y) \chi_{l_1 l_2}^* \quad (2.25)$$

$$\begin{aligned} \tilde{f}_{l_1 l_2}^{(2)} = & \int_0^\pi dy (1 - \cos y) \left\{ \int_\pi^{2\pi-y} F(x - 2\pi, y) + \int_{-\pi}^\pi F(x, y) \right. \\ & \left. + \int_{-2\pi+y}^{-\pi} F(x + 2\pi, y) \right\} \chi_{l_1 l_2}^*(x, y) dx. \end{aligned} \quad (2.26)$$

Two typical examples are presented below.

Example 1 .

When $F(x, y) = e^{i\alpha x}$, i.e., pure imaginary action, l_1 is limited to even integer since l_2 is zero.

$$\tilde{f}_{l_1 0} = \int d\Omega F(x, y) \chi_{l_1 0}^*(x, y) \quad (2.27)$$

Then

$$\begin{cases} \tilde{f}_{l_1 0}^{(1)} = \frac{1}{8\pi^2} \int_\pi^{2\pi} dy (1 - \cos y) \int_{-2\pi+y}^{2\pi-y} dx e^{i\alpha x - i\frac{l_1}{2}x} \\ \tilde{f}_{l_1 0}^{(2)} = \frac{1}{8\pi^2} \int_0^\pi dy (1 - \cos y) \left\{ \int_\pi^{2\pi-y} dx e^{i\alpha(x-2\pi)} e^{-il_1 x/2} \right. \\ \left. + \int_{-\pi}^\pi dx e^{i\alpha x} e^{-il_1 x/2} + \int_{-2\pi+y}^{-\pi} dx e^{i\alpha(x+2\pi)} e^{-il_1 x/2} \right\} \end{cases} \quad (2.28)$$

which gives

$$\begin{cases} \tilde{f}_{l_1 0}^{(1)} = \frac{1}{8\pi^2} \int_0^\pi dy (1 - \cos y) \int_{-y}^y dx e^{i(\alpha - \frac{l_1}{2})x} \\ \tilde{f}_{l_1 0}^{(2)} = \frac{1}{8\pi^2} \int_0^\pi dy (1 - \cos y) \left\{ 2 \int_{-\pi}^\pi dx e^{i(\alpha - \frac{l_1}{2})x} - \int_{-y}^y dx e^{i(\alpha - \frac{l_1}{2})x} \right\}. \end{cases} \quad (2.29)$$

And finally we obtain

$$\begin{aligned} \tilde{f}_{l_1 0} &= \tilde{f}_{l_1 0}^{(1)} + \tilde{f}_{l_1 0}^{(2)} \\ &= \frac{1}{4\pi^2} \int_0^\pi dy (1 - \cos y) \int_{-\pi}^\pi dx e^{i(\alpha - \frac{l_1}{2})x} \\ &= \frac{1}{2\pi} \frac{1}{\alpha - \frac{l_1}{2}} \sin\left(\left(\alpha - \frac{l_1}{2}\right)\pi\right) \\ &= A_{l_1}(\alpha). \end{aligned} \quad (\text{II})$$

This is just the same form as the one obtained in U(1) gauge theory with pure θ -term.

Example 2 .

For

$$F(x, y) = "x" = \begin{cases} x - 2\pi & \text{for } \pi \leq x \leq 2\pi \\ x & \text{for } -\pi \leq x \leq \pi \\ x + 2\pi & \text{for } -2\pi \leq x \leq -\pi, \end{cases} \quad (2.30)$$

$$\tilde{f}_{l0} = \frac{2}{i} \frac{dA_l(\alpha)}{d\alpha} \Big|_{\alpha=0} \quad (2.31)$$

where $A_l(\alpha)$ is defined in the above example 1. We have

$$\tilde{f}_{l0} = \begin{cases} 0 & \text{for } l = 0 \\ \frac{2i}{l} (-1)^{\frac{l}{2}} & \text{for } l \neq 0, l = \text{even}. \end{cases} \quad (\text{III})$$

This coincides with the result (I).

§3. Results

We adopt fundamental representation as the bare real action, i.e., Wilson action and “standard θ -term action” as the bare imaginary action.

$$F = \exp\{\beta(\cos \phi_1 + \cos \phi_2 - 2) + i\alpha(\phi_1 + \phi_2)\}, \quad (3.1)$$

where β denotes β_{11} since

$$\chi_{11} = e^{i\frac{\pi}{2}} 2 \cos \frac{y}{2} \quad (3.2)$$

$$\chi_{11} + \chi_{11}^* = 4 \cos \frac{x}{2} \cos \frac{y}{2} = 2(\cos \phi_1 + \cos \phi_2). \quad (3.3)$$

This bare action contains both U(1) and SU(2) part in the real action and only U(1) part in the imaginary action. Although SU(2) part is not contained in the imaginary action at bare level, renormalization transformation leads to SU(2) part also in the imaginary action as a consequence of interference between real and imaginary action.

§3.1 $\alpha = 0$ ($\theta = 0$) case (pure real action)

When $\alpha = 0$ ($\theta = 0$) we have simple form of character expansion coefficients,

$$F = \sum_{l_1+l_2=\text{even}} \tilde{f}_{l_1 l_2} \chi_{l_1 l_2}(x, y) d_{l_1 l_2} \quad (3.4)$$

$$\tilde{f}_{l_1 l_2} = \frac{e^{-2\beta}}{d_{l_1 l_2}} \det_{ij} (I_{\lambda_i - i + j}(\beta)), \quad (3.5)$$

where

$$\begin{cases} \lambda_1 = (l_1 + l_2)/2 \\ \lambda_2 = (l_1 - l_2)/2. \end{cases} \quad (3.6)$$

and $I_n(\beta)$ denotes the Modified Bessel functions.

Bare action contains $\beta_{11}^b \neq 0$, others=0. As the result of renormalization transformation all coefficients $\beta_{l_1 l_2}^r$ (renormalized) appear. We pick up (β_{11}, β_{22}) from these infinite dimensional coupling constant space. The renormalization flow starting from various bare couplings converges to a trajectory in (β_{11}, β_{22}) plane (Fig. 1 and Fig. 2).

Fig. 1

Fig. 2

They approach so called heat kernel [21]. In the weak coupling limit ($\beta \rightarrow \infty$), modified Bessel function is given by

$$I_n(\beta) \sim \frac{e^\beta}{\sqrt{2\pi\beta}} e^{-\frac{n^2}{2\beta}} \quad (3.7)$$

and we have in the case of U(2) gauge group, with the use of (3.5),

$$F_{\text{U}(2)}^{h.k.} = \sum_{l_1+l_2=\text{even}} d_{l_1 l_2} \chi_{l_1 l_2} \tilde{f}_{l_1 l_2}^{h.k.} = \sum d_{l_1 l_2} \chi_{l_1 l_2} e^{-\frac{1}{2\beta}(\frac{1}{2}l_1^2 + l_2(\frac{l_2}{2} + 1))} / 2\pi\beta^2 \quad (3.8)$$

Namely,

$$\begin{aligned} F_{\text{U}(2)}^{h.k.} &= \sum_{l_1, l_2 \text{ all}} \frac{1}{2} (1 + (-1)^{l_1 + l_2}) d_{l_1 l_2} \chi_{l_1 l_2}(x, y) \tilde{f}_{l_1 l_2}^{h.k.} \\ &= \sum_{l_1, l_2 \text{ all}} \sum_{\nu=0}^1 d_{l_1 l_2} \frac{1}{2} e^{i l_1 x_\nu / 2} \frac{\sin(l_2 + 1) \frac{y_\nu}{2}}{\sin \frac{y_\nu}{2}} \times e^{-\frac{1}{2\beta} C_{l_1 l_2}} \end{aligned} \quad (3.9)$$

where

$$\begin{cases} x_\nu = x + 2\pi\nu, \\ y_\nu = y - 2\pi\nu, \end{cases} \quad (3.10)$$

with $\nu = 0, 1$.

In this way the character expansion coefficient is written as

$$\tilde{f}_{l_1 l_2}^{h.k.} = \frac{1}{2\pi\beta^2} e^{-\frac{1}{2\beta} C_{l_1 l_2}} \quad (3.11)$$

where

$$C_{l_1 l_2} = \text{quadratic Casimir operator of } U(2) = \frac{1}{2}l_1^2 + l_2\left(\frac{l_2}{2} + 1\right). \quad (3.12)$$

In strong coupling region, heat kernel (3.9) gives the relation between coupling constants. For example we have

$$\beta_{22} \sim -\frac{3}{8}\beta_{11}^2 \quad (3.13)$$

at $\beta \ll 1$. In Fig. 1 and Fig. 2, coupling constant relation obtained by heat kernel (3.9) is shown. The actual trajectory in strong coupling region is quite close to (3.13).

After t steps of renormalization transformation

$$F^{h.k.}(\lambda^t a, x, y) = \sum_{l_1+l_2=\text{even}} d_{l_1 l_2} \chi_{l_1 l_2}(x, y) (\tilde{f}_{l_1 l_2}^{h.k.})^{\lambda^{2t}} \quad (3.14)$$

$$(\tilde{f}_{l_1 l_2}^{h.k.})^{\lambda^{2t}} \propto e^{-\frac{\lambda^{2t}}{2\beta(a)} C_{l_1 l_2}} \equiv e^{-\frac{1}{2\beta(\lambda^t a)} C_{l_1 l_2}} \quad (3.15)$$

Namely, coupling constant β in heat kernel is transformed, after t steps of renormalization transformation, to simply β/λ^{2t} , (at each transformation β is divided by λ^2), i.e., the functional form is not changed but only the value of β is changed.

§3.2 $\alpha \neq 0$ ($\theta \neq 0$) case(imaginary action)

We introduce standard θ -term action as the bare action. In this case bare imaginary coupling constants are

$$\gamma_{l_1 0}^b = \frac{i(-1)^{l_1/2}}{l_1} 2\alpha, \quad \gamma_{00}^b = 0, \quad \gamma_{l_1 l_2}^b = 0 \text{ for } l_2 \neq 0. \quad (3.16)$$

Then renormalized couplings are non zero, $\gamma_{l_1 l_2}^r \neq 0$ even for $l_2 \neq 0$, e.g., γ_{11}, γ_{22} etc. are induced by renormalization effects through interference between β_{11} and $\gamma_{l_1 0}$.

In the following, some characteristics of the RG flow will be discussed in detail.

- 1) (β_{11}, β_{22}) flow; The flow projected onto (β_{11}, β_{22}) plane depends on bare θ , but flows starting from different β converge to a unique trajectory independently of bare parameters. As θ approaches π , trajectory is much affected by the fixed point $\theta = \pi$. The trajectory, however, does not stay at finite (β_{11}, β_{22}) , but finally approaches the strong coupling limit $(0, 0)$ at large t (= RG transformation step) . It shows that the charge of fundamental representation of U(2) group is in the confinement phase even at $\theta = \pi$. Main reason is that SU(2) part of U(2) plays important role for the charge of fundamental representation.

Fig. 3

- 2) (β_{20}, β_{40}) flow; Originally $\beta_{l_1 0}^b = 0$ for all l_1 in our set of bare parameters. These $(\beta_{l_1 0}^r)$'s are induced by RG transformation. In the first t steps ($< t_0$), which we call region I, renormalized couplings $(\beta_{20}^r, \beta_{40}^r)$ are strongly affected by the fixed point ($\theta = \pi$). As we change bare θ , the influence of the fixed point becomes stronger as θ approaches π . After t_0 steps, flows start to move to infrared fixed point $(\beta_{20}^r, \beta_{40}^r) = (0, 0)$ for $\theta^b \neq \pi$. At $\theta = \pi$, $(\beta_{20}^r, \beta_{40}^r)$ approaches fixed point $(1/2, -1/4)$ as $t \rightarrow$ large. Namely, at $\theta = \pi$, only region I exists but region II does not.

Fig. 4

We have from eq.(II) in section 2,

$$\tilde{f}_{00}(\alpha) = \tilde{f}_{20}(\alpha) \tag{3.17}$$

when $\alpha = \frac{1}{2}(\theta = \pi)$. The other coefficients are smaller than these two.

$$\tilde{f}_{00}\left(\frac{1}{2}\right) = \tilde{f}_{20}\left(\frac{1}{2}\right) > \tilde{f}_{-20}\left(\frac{1}{2}\right) = \tilde{f}_{40}\left(\frac{1}{2}\right) > \dots \tag{3.18}$$

and RG transformation leads to the result that large distance behavior is dominated by $\tilde{f}_{00} = \tilde{f}_{20}$ for $\alpha = 1/2$.

$$F \sim \tilde{f}_{00}^{\lambda^{2t}} (1 + e^{ix}) \propto 2 \cos \frac{x}{2} e^{i\frac{x}{2}} \quad (3.19)$$

at $t \rightarrow \infty$ and $\lambda > 1$. This gives

$$\begin{aligned} s &= \ln(2 \cos \frac{x}{2}) \\ v &= \frac{x}{2}. \end{aligned} \quad (3.20)$$

Renormalized θ -term action is exactly given by $\frac{1}{2}x$ (fixed point action). Namely, for $\alpha^b = 1/2$, RG flow in (β_{20}, β_{40}) plane converges to $(\frac{1}{2}, \frac{-1}{4})$ point, because fixed point action $s = \ln(2 \cos \frac{x}{2})$ leads to $\beta_{l_1 0} = \frac{2}{|l_1|} (-1)^{\frac{l_1}{2}+1} (l_1 \neq 0)$.

Charge in $(2, 0)$ representation is deconfined at $\theta = \pi$ by θ - term. (In pure U(1) theory we showed fundamental representation charge is deconfined.) θ -term works as the back ground field to the U(1) part of U(2) group and background field just cancels the electric field produced by the U(1) charge of Wilson loop.

3) $(\text{Im}\gamma_{11}, \beta_{11})$ flow; Originally $\gamma_{11} = 0$, i.e., the coupling with nontrivial SU(2) part was absent in the bare action. The coupling γ_{11} is induced as RG effect for nonzero θ 's ($0 < \theta < \pi$), while γ_{11} is zero for $\theta = 0$. Only small $|\gamma_{11}^r|$ is induced for $\theta \rightarrow \pi$. For $\theta^b = \pi$, $\gamma_{11}^r = 0$, because at $\theta = \pi$, θ -term remains fixed point. In that case $\gamma_{l_1 0}^r \equiv \frac{2^i}{l_1} (-1)^{l_1/2}$, and, $\gamma_{l_1 l_2}^r = 0$ for all $l_2 \neq 0$. In Fig. 5. $(\text{Im}\gamma_{11}, \beta_{11})$ flow is shown in Fig. 5.

Fig. 5

4) string tension; The string tension is defined by

$$\sigma_{l_1, l_2} = -\frac{1}{L^2} \ln \frac{\int d\Omega \chi_{l_1, l_2}^*(u) F(L, u)}{\int d\Omega F(L, u)} \quad (3.21)$$

The string tension with nontrivial SU(2) part, i.e., string tension σ_{11} coming from the Wilson loop of IR(irreducible representation) $(l_1, l_2) = (1, 1)$, decreases as θ approaches π and $\sigma_{11} \rightarrow$ finite as $\theta \rightarrow \pi$. String tension for representation $(2, 0)$ Wilson loop, i.e., string tension with trivial SU(2) part, $\sigma_{2,0} \rightarrow 0$ as $\theta \rightarrow \pi$. This again shows that $(2, 0)$ charge is deconfined at $\theta = \pi$ but $(1, 1)$ is not even at

$\theta = \pi$. In the latter case, SU(2) part drives the system always to the confinement phase.

Free energy is also shown. Free energy is

$$-\{\ln \int d\Omega F(L, u)\}/L^2 \quad (3.22)$$

It is nearly proportional to θ^2 .

Fig. 6(a), (b)

- 5) ($\text{Im}\gamma_{20}, \text{Im}\gamma_{40}$) flow; Qualitative difference is seen between $t < t_0$ (region I), and $t > t_0$ (region II). It is attracted by the $\theta = \pi$ fixed point and moves very slowly due to this attraction for $t < t_0$. Note that the flow for this pair of couplings starts from the nearest point to $\theta = \pi$ fixed point. It moves on a parabola to $(\gamma_{20}, \gamma_{40}) = (0, 0)$ fixed point for $t > t_0$. Flows for various θ are plotted in Fig. 7. At $\theta = 0.999\pi$ the flow is strongly attracted to the $\theta = \pi$ fixed point and stays rather long time near this point(region I), but finally trajectory moves toward $(0, 0)$ fixed point(region II). For $\theta = \pi$ bare theory, RG flow does not move at all(the system is always in region I) and $(\text{Im}\gamma_{20}, \text{Im}\gamma_{40})$ stays at $(-\frac{1}{2}, \frac{1}{4})$

Fig. 7

- 6) ($\text{Im}\gamma_{11}, \text{Im}\gamma_{22}$) flow; Originally the value of $(\gamma_{11}, \gamma_{22})$ is $(0, 0)$. But they(γ_{11} and γ_{22}) are induced by RG transformation by the interference between real β_{11} Wilson term and imaginary $\gamma_{l,0}$'s. As seen in Fig. 8, the flow starts from $(0, 0)$ point and $|\text{Im}\gamma_{11}|$ and $|\text{Im}\gamma_{22}|$ becomes lager, in region I and then get back to the strong coupling fixed point(region II).

Fig. 8

- 7) Change of θ -term under RG; In this paper we adopted “standard ” action for imaginary(θ)-term.As in Fig. 9, originally the imaginary action is given by linear dependence on x with $\theta^b = 0.8\pi$ in eq.(2.20). But after RG transformation, the shape of the potential changes. In the first several steps (Region

I), the shape still reflects the original form, but after t_0 steps, the shape approaches sine curve, which is expected because imaginary coupling of higher IR(irreducible representation) dumps much faster than the lowest IR one, e.g., $\text{Im}\gamma_{40} \sim (\text{Im}\gamma_{20})^2 \ll |\text{Im}\gamma_{20}| \ll 1$ for any $\theta^b (\neq 0 \text{ or } \pi)$.

On the other hand, when $\theta^b = \pi$, the shape of $v(x)$ does not change(as is seen in eqs.(3. 17)~ (3.20)).

Fig. 9

§4. Conclusions and discussions

Migdal Renormalization Group method is applied to U(2) gauge theory with θ -term in two space-time dimensions. This system is described by two group variables x and y , corresponding to U(1) part and diagonal SU(2) part of U(2) group respectively.

For each θ -parameter, various bare real couplings lead to a unique trajectory, heat kernel. The trajectory differs, however, depending on bare θ^b 's.

Bare action is chosen in this paper such that

- 1) real part of the action is given by Wilson action corresponding to the fundamental representation, i.e., the bare coupling is given by β_{11}^b , and all the others are set to be zero.
- 2) imaginary(θ -term) action is given by “standard θ -term action”,

$$v(x) = \alpha x$$

which contains only U(1) variable x and

$$\gamma_{l_1 l_2}^b (l_2 \neq 0) = 0.$$

Starting from this bare action, imaginary couplings with non trivial SU(2) representations are induced as a result of RG transformations, i.e., due to the interference between β_{11} and $\gamma_{l_1 0}$'s.

The imaginary couplings with nontrivial SU(2) part($l_2 \neq 0$), however go to zero finally after many steps of RG transformation, which will be related to the

fact that the real couplings with nontrivial SU(2) part finally go to zero infrared fixed point for any θ -parameter even for π .

Real couplings are affected by the imaginary (θ -term) couplings.

- (i) $\beta_{l_1 0}$'s (any l_1) go to non zero fixed point for $\theta^b = \pi$. These couplings even for $\theta^b \neq \pi$ are first attracted by the fixed point due to $\theta = \pi$ in the first several RG steps. Spending some RG steps around it, they finally start to move to the infrared fixed point $\beta_{l_1 0} = 0$ when $\theta^b \neq \pi$. The string tension σ_{20} coming from the Wilson loop in the IR(2, 0) tends to zero as $\theta^b \rightarrow \pi$. It means the system undergoes deconfinement phase transition at $\theta = \pi$.
- (ii) Even for $\theta^b \rightarrow \pi$, $\beta_{l_1 l_2}$ ($l_2 \neq 0$) goes to strong coupling limit ($\beta_{l_1 l_2} \rightarrow 0$). We also saw that σ_{11} does not go to zero but to a finite value. It means IR(1, 1) does not undergo deconfinement phase transition due to the influence of SU(2) part.

As the future problems,

1. The RG study of CP^{N-1} system with θ -term in 2 space-time dimensions will be quite interesting. It should be made clear whether θ_c depends on bare real coupling β^b and whether θ_c will move to smaller values as $\beta^b \rightarrow$ large.
2. Renormalization group study about four dimensional gauge systems (Z_N or U(1)) with θ -term will be interesting. To study the rich phase structure conjectured by Cardy and Rabinovic based on the free energy argument should be confirmed by RG method or numerical simulations.

Acknowledgements

The authors are grateful to members of Theory group at Kyushu University for discussions. This work is supported by Grant-in-Aid (C) No.08640381(Masahiro Imachi) and No.07640417 (Hiroshi Yoneyama) from the Ministry of Education, Science, Sports and Culture.

Figure Captions

- Fig. 1. RG flow of real coupling constants for $\theta = 0$. Bare couplings are $\beta_{11}^b = 1, \dots, 8$. Every flow converges a unique trajectory at second step(scale parameter is chosen in this paper as $\lambda^2 = 2$). Heat kernel is also shown. Renormalized coupling is close to heat kernel couplings.
- Fig. 2. The same as Fig. 1. Flow in strong coupling region is shown. Independent of bare couplings, all the points lie on a unique trajectory.
- Fig. 3. Flows for nonzero θ 's are shown. Bare couplings are $\beta_{11}^b = 4$ and 6 , $\theta = 0.8\pi$ and 1.0π . Trajectory depends on bare θ but independent of bare β for each θ .
- Fig. 4. Flow of couplings of U(1) part. Thick line, dashed line and thin line denotes $\theta = 0.8\pi, \theta = 0.999\pi$ and 1.0π , respectively. At first(region I) they are attracted by the fixed point $\beta_{20} = 1/2, \beta_{40} = -1/4$, controlled by $\theta = \pi$. After spending several steps(t_0), they start to move(region II) to infrared fixed point $\beta_{20} = 0, \beta_{40} = 0$. The influence of $\theta = \pi$ fixed point is stronger for bare θ close to π .
- Fig. 5. Flow of couplings of nontrivial representation of SU(2). Coupling γ_{11} , originally zero, acquires nonzero values due to RG effect. It, however, goes to zero by the effect of SU(2) confinement fixed point.
- Fig. 6(a). String tensions, σ_{20} (bold line) and σ_{11} (thin line) , are shown for various bare θ . σ_{20} goes to zero at $\theta = \pi$. It shows IR (2, 0) is deconfined by the back ground electric field coming from θ -term. σ_{11} approaches non zero value even at $\theta = \pi$. It shows IR(1, 1) belongs to non trivial SU(2) representation and stays always in confinement phase, since there is no back ground field contributing to SU(2) part.
- Fig. 6(b). Free energy vs. θ . It is proportional to θ^2 .
- Fig. 7. Flow of imaginary couplings of U(1) part. Bare θ are 0.8π and 0.999π . At first several RG steps(region I), renormalized couplings are attracted by the non trivial fixed point($\theta = \pi$). Staying at the starting point for a number of steps, they then begin to move to infrared fixed point. The effect of the nontrivial fixed point is stronger for θ near to π .

Fig. 8. Flow of imaginary couplings, $\text{Im}\gamma_{11}$ and $\text{Im}\gamma_{22}$, with nontrivial $\text{SU}(2)$ part. In region I, absolute values of them increase but they move to infrared fixed point finally.

Fig. 9. Change of shape of imaginary action under RG transformations. Here t denotes the number of steps of renormalization group transformation. At first, linear x dependence is clear, but afterwards shape changes to sine curve. This is due to the fact that only single IR(the lowest representation) survives in strong coupling regions.

References

- [1] G. 't Hooft, Nucl. Phys. **B190**[FS3](1981)455.
- [2] J. L. Cardy and E. Rabinovici, Nucl. Phys. **B205**[FS5](1982)1.
- [3] J. L. Cardy, Nucl. Phys. **B205**[FS5](1982)17.
- [4] E. Fradkin and F. A. Shaposnik, Phys. Rev. Lett. **66**(1991)267.
- [5] S. Coleman, Ann. Phys. **101**(1976)239.
- [6] A. S. Hassan, M. Imachi and H. Yoneyama, Prog. Theor. Phys. **93**(1995)161.
- [7] A. S. Hassan, M. Imachi, N.Tsuzuki and H. Yoneyama, Prog. Theor. Phys. **94**(1995)861.
- [8] A. S. Hassan, M. Imachi, N.Tsuzuki and H. Yoneyama, Prog. Theor. Phys. **95**(1996)175.
- [9] U. -J. Wiese, Nucl. Phys. **B318**(1989)153.
- [10] G. Schierholz, “ θ Vacua, Confinement and The Continuum Limit”, preprint DESY 94-229, HLRZ 94-63.
- [11] G. Schierholz, hep-lat/9409019.
- [12] U. -J. Wiese, Nucl. Phys. **B318**(1989)153.
- [13] A. A. Migdal, Sov. Phys. JETP **42**(1976)413, 743.
- [14] L. P. Kadanoff, Ann. Phys. **100**(1976)359.
- [15] K. M. Bitar, S. Gottlieb and C. K. Zachos, Phys. Rev. **26**(1982)2853, Phys. Lett. **B121**(1983)163.
- [16] M. Imachi, S. Kawabe and H. Yoneyama, Prog. Theor. Phys. **69**(1983)221, 1005.
- [17] K. G. Wilson and J. B. Kogut, Phys. Rep. **12C**(1974) 75.
- [18] T. G. Kovacs, E. T. Tomboulis and Z. Schram, Nucl. Phys. **B454**(1995)45.
- [19] J-M. Drouffe and J-B.Zuber, Phys. Rep. **102**(1983) 1.
- [20] H. Weyl, “The Classical Group”(Princeton Univ. Press(1939).
- [21] P. M. Menotti and E. Onofri, Nucl. Phys. **B190**[FS3](1981)288.

Figure 1

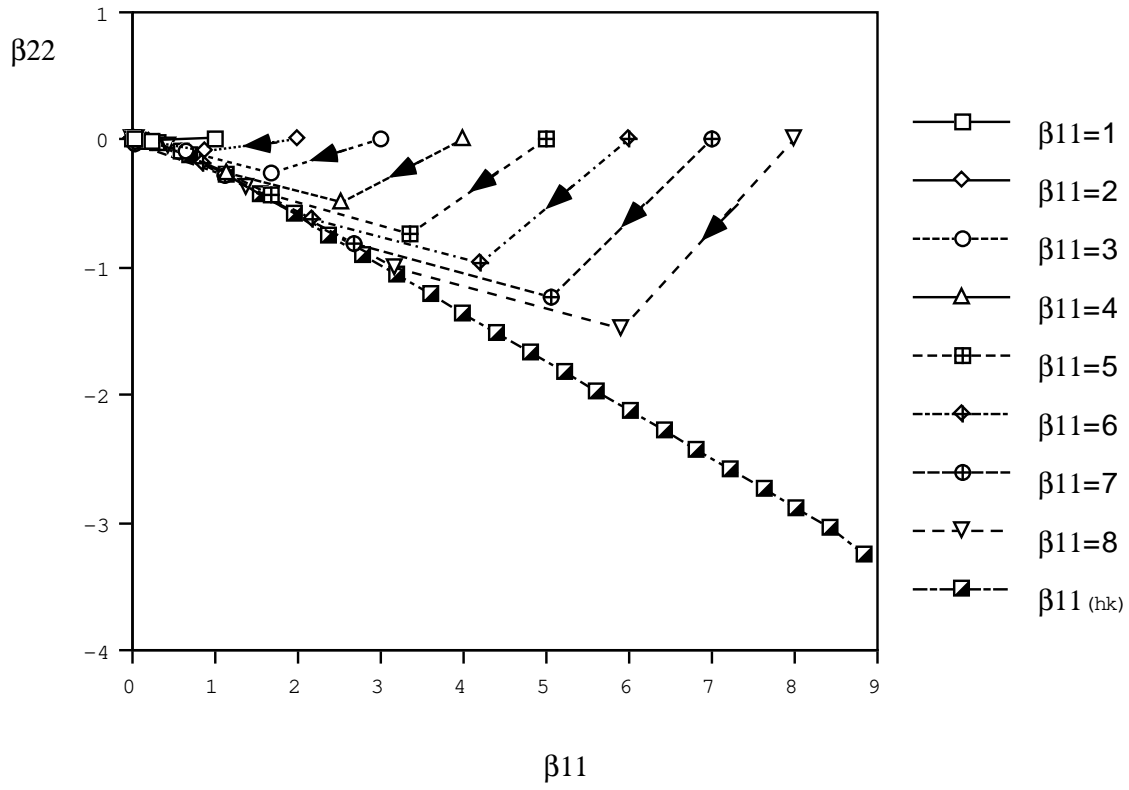


Figure 2

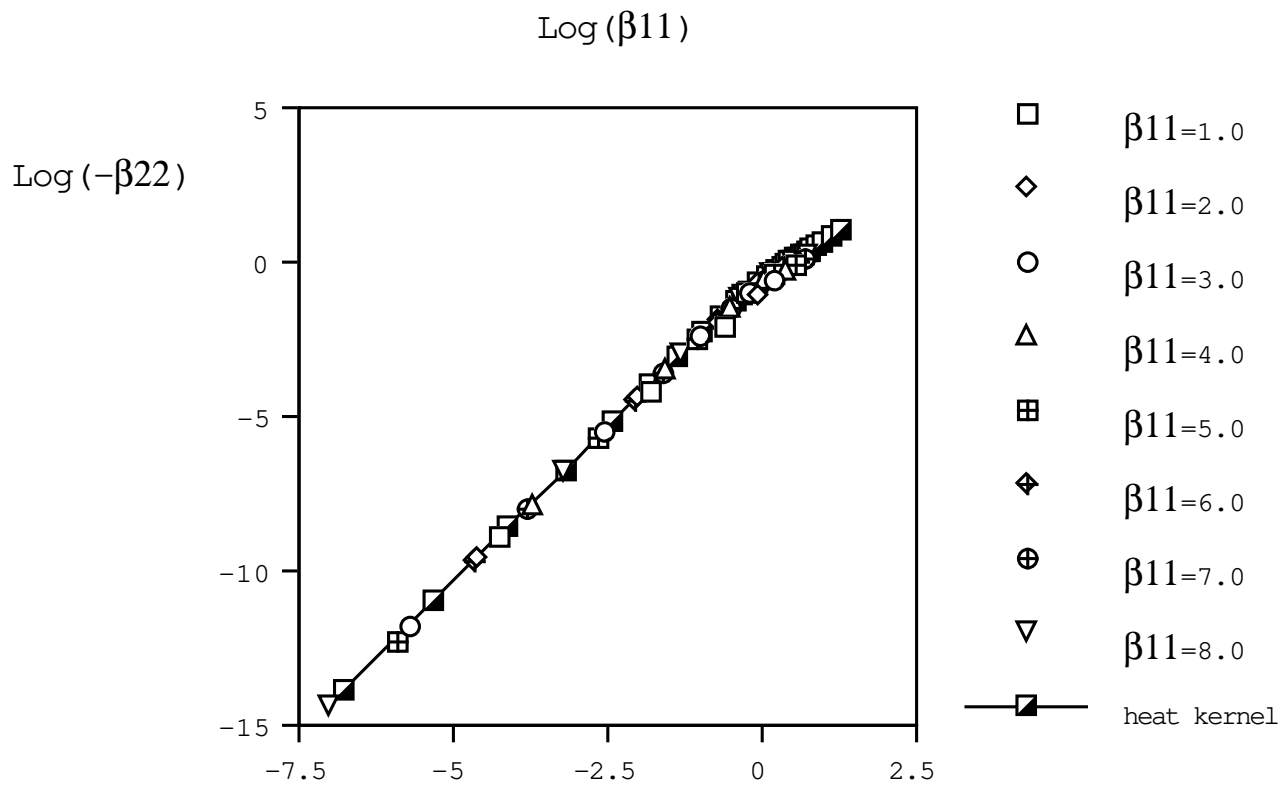


Figure 3

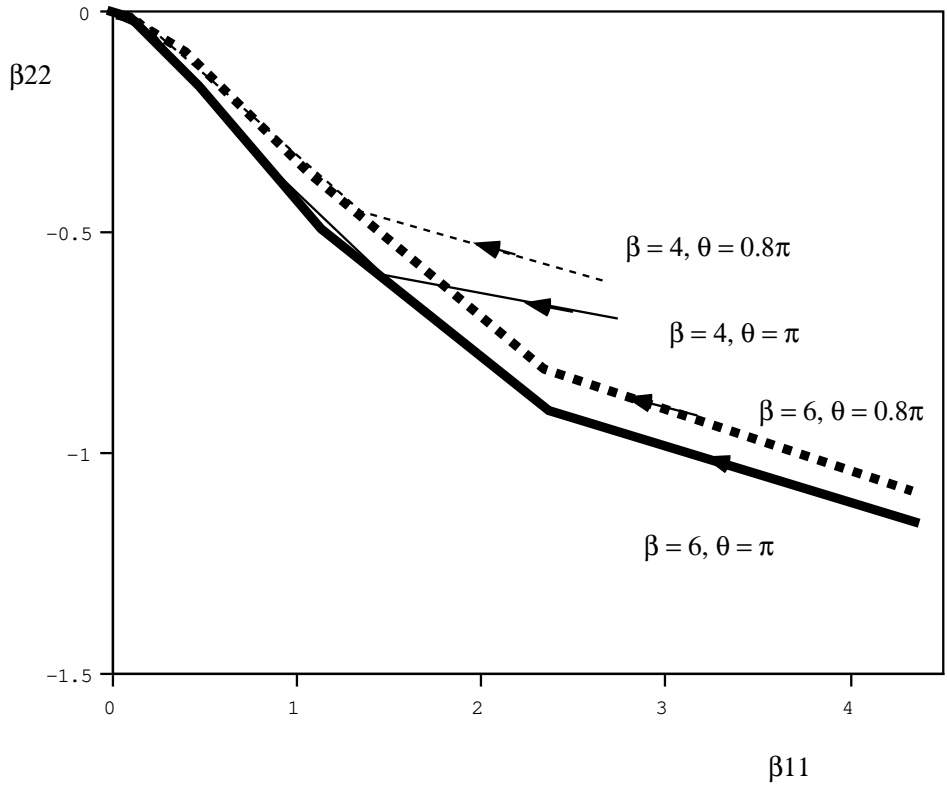


Figure 4

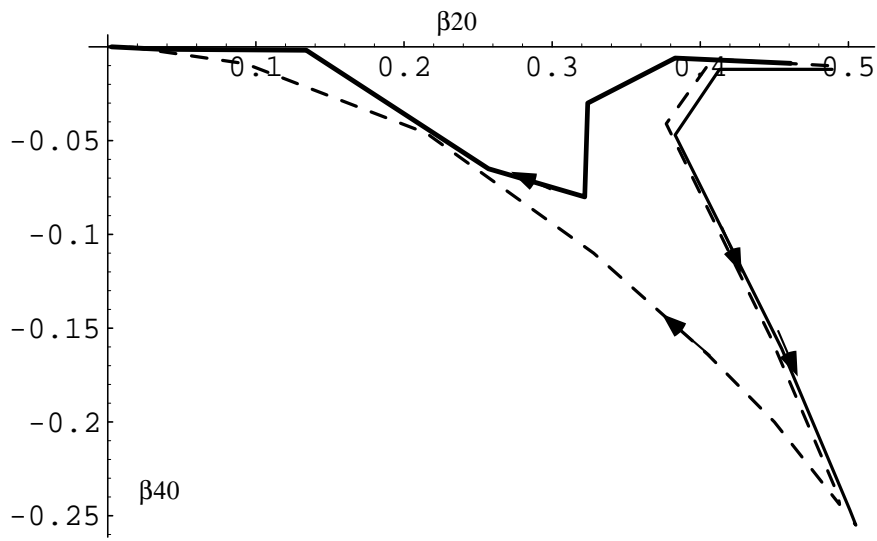


Figure 5

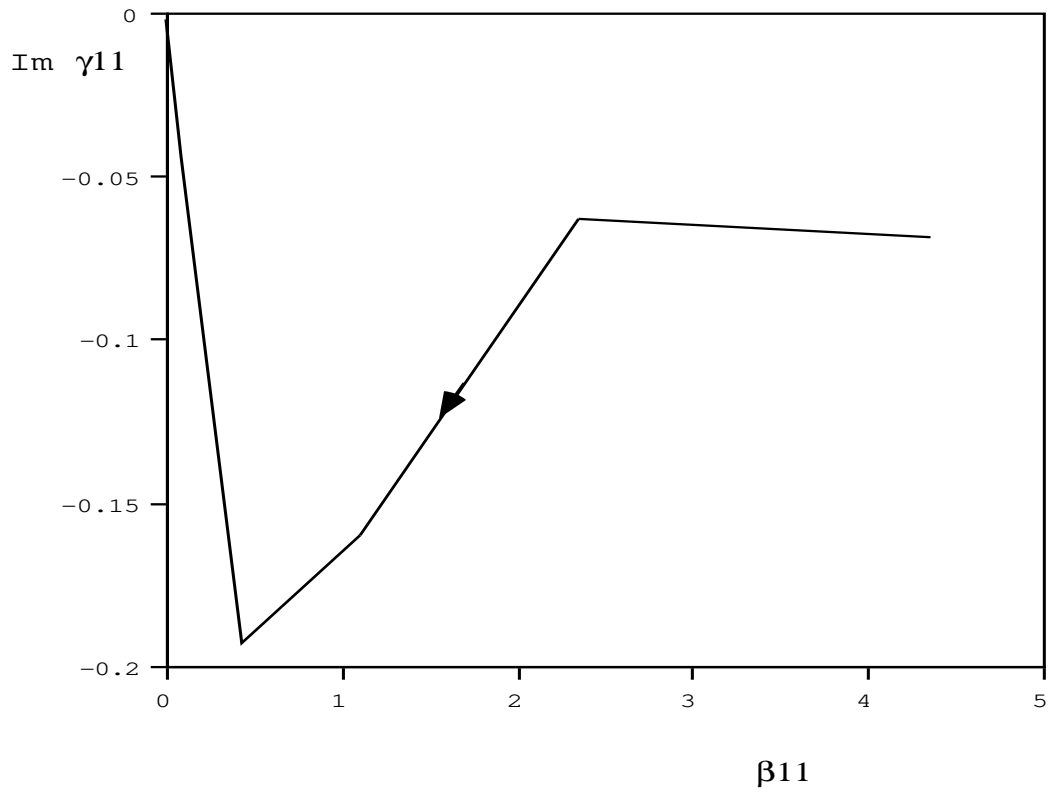


Figure 6(a)

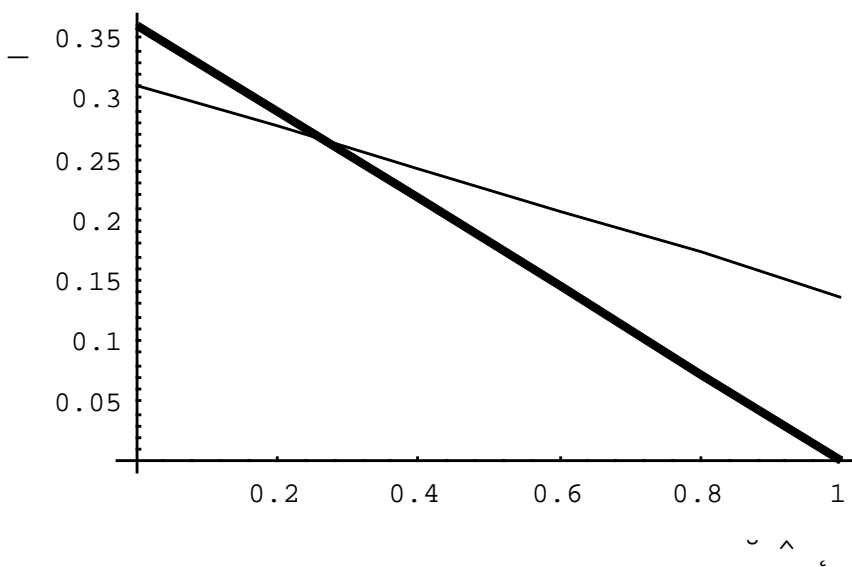


Fig. 6(b)

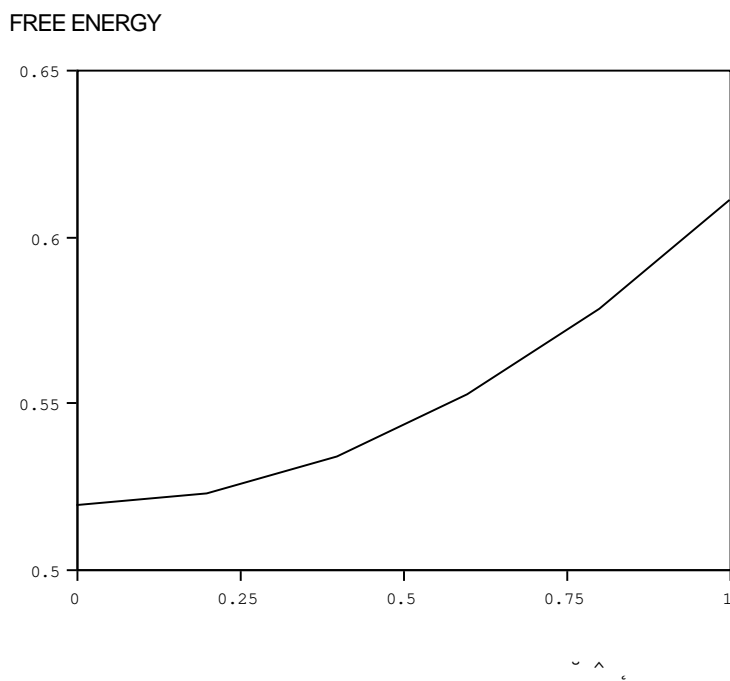


Figure 7

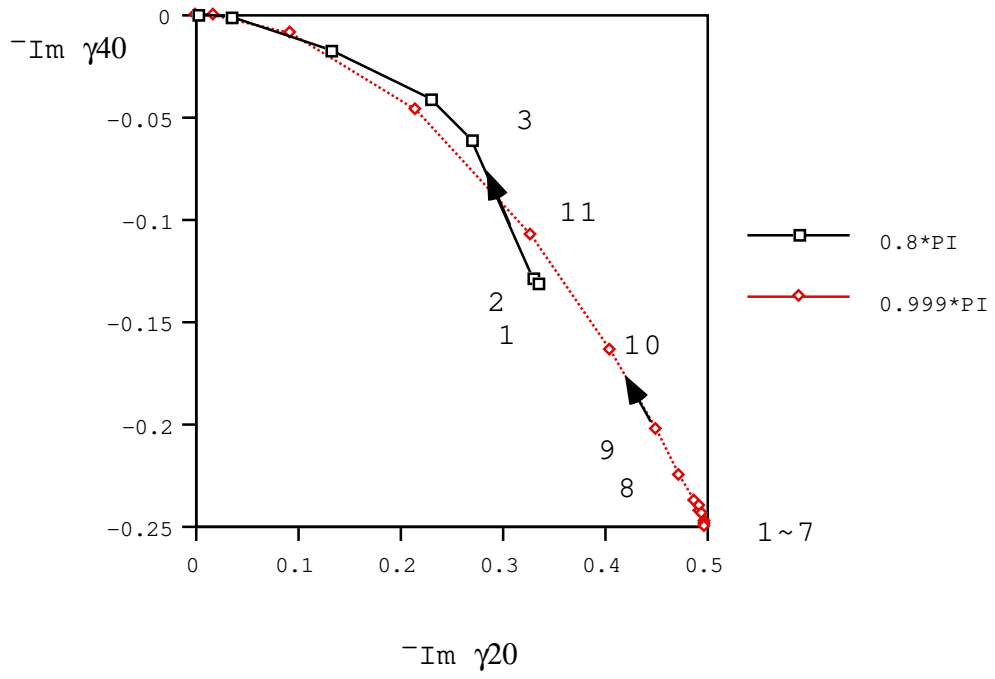


Figure 8

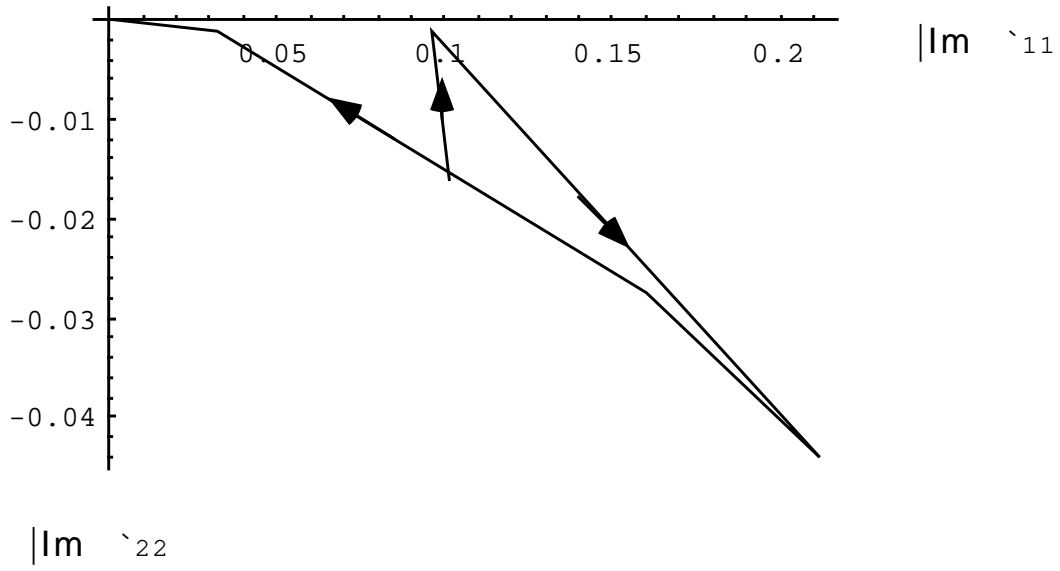


Figure 9

